# Joint probability of precipitation and discharge deficits in the Netherlands

Jules J. Beersma and T. Adri Buishand

Royal Netherlands Meteorological Institute, De Bilt, The Netherlands

Received 14 April 2004; revised 20 August 2004; accepted 28 September 2004; published 15 December 2004.

[1] The Netherlands are situated at the downstream end of the Rhine River. A large part of the country can be supplied with water from the river in the case of precipitation deficits. For drought assessment it is therefore necessary to consider the joint distribution of precipitation and discharge deficits. A transformed bivariate normal distribution as well as a bivariate Gumbel distribution are fitted to this data. In addition, nearest-neighbor resampling is used to estimate joint probabilities of precipitation and discharge deficits. Both the reproduction of the marginal distributions and the dependence structure are explored. It is found that the transformed bivariate normal distribution underestimates the probability that both the precipitation and discharge deficit are extreme due to its asymptotic independence. Nearest-neighbor resampling also underestimates this probability, mainly because the upper tails of the marginal distributions are not properly reproduced by the simulations. From the two fitted bivariate distributions a novel bivariate distribution is constructed with transformed normal marginals and a logistic Gumbel dependence structure, which gives the best description of the upper tail of the joint distribution. The use of a failure region based on economic damage rather than on joint exceedances considerably reduces the differences between the probabilities of drought from the various bivariate models. *INDEX TERMS:* 1812 Hydrology: Drought; 1818 Hydrology: Evapotranspiration; 1854 Hydrology: Precipitation (3354); 1860 Hydrology: Runoff and streamflow; *KEYWORDS:* bivariate distributions, dependence structure, economic damage, failure region, nearest-neighbor resampling, precipitation and discharge deficits

**Citation:** Beersma, J. J., and T. A. Buishand (2004), Joint probability of precipitation and discharge deficits in the Netherlands, *Water Resour. Res.*, *40*, W12508, doi:10.1029/2004WR003265.

## 1. Introduction

[2] A large part of the Netherlands is situated in the delta of the Rhine River, the largest river in northwestern Europe (drainage area 185 000 km$^2$). The Rhine rises in the Swiss Alps and flows via France and Germany to the Netherlands, where it divides a number of times. The Rhine plays a major role in the overall water balance of the Netherlands; the amount of Rhine water that flows through the Netherlands is on average twice as large as the amount that the country receives as precipitation [*Middelkoop and van Haselen*, 1999]. As a result, large parts of the country can be supplied with water from the river in the case of precipitation deficits.

[3] This paper addresses the probability of drought in the Netherlands. For droughts with a large economic impact, it is important to consider the joint distribution of the precipitation deficit in the Netherlands and the discharge deficit of the Rhine River. Two approaches are compared to estimate joint probabilities: (1) fitting bivariate distributions to the historical data, and (2) time series simulation.

[4] In the first approach a transformed bivariate normal distribution and a limiting bivariate Gumbel distribution are used. Both bivariate distributions have been applied in the water resources literature [*Leytham*, 1987; *Kroll and Stedinger*, 1998; *Yue et al.*, 1999; *Yue*, 2001; *Shiau*, 2003], but a thorough comparison is lacking. Apart from differences between the marginal distributions, the dependence structure of a limiting bivariate Gumbel distribution is quite different from that of the classical bivariate normal distribution, in particular regarding the joint occurrence of large values. To assess the suitability of the dependence structure of these bivariate distributions new diagnostics from the statistical literature on multivariate extremes [*Ledford and Tawn*, 1996; *Coles et al.*, 1999] are used. The adequacy of the fit of the bivariate distributions is further explored by comparing theoretical and empirical joint exceedance probabilities. In the second approach nearest-neighbor resampling is used to generate a long sequence ($10^5$ years) of precipitation and discharge deficits. This resampling technique has successfully been applied to simulate time series of river flows [*Lall and Sharma*, 1996] and weather variables [*Young*, 1994; *Rajagopalan and Lall*, 1999; *Buishand and Brandsma*, 2001]. In the nearest-neighbor resampling procedure the variables of interest (which in our case include precipitation, evaporation and river discharge) are sampled simultaneously with replacement from the historical data. A convenient characteristic of resampling is that no assumptions have to be made about the underlying


0043-1397/04/2004WR003265$09.00

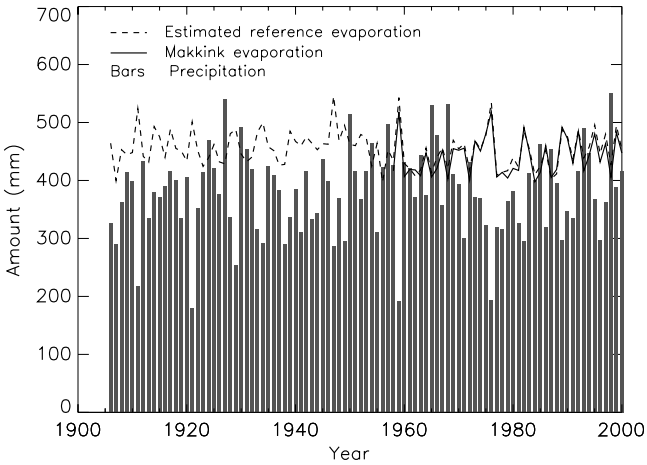


**Figure 1.** Evaporation and precipitation in the Netherlands in the summer half-year (April–September) for the period 1906–2000. Estimated reference and Makkink evaporation are explained in the text.

distributions of each of the variables and of the dependencies between those variables.

[5] The sensitivity of joint probabilities to the form of the marginal distributions and the dependence structure is discussed. Besides the probability of joint exceedances, attention is given to the probability associated with a failure region based on economic damage.

[6] In Section 2 the historical data are described, and the precipitation deficit in the Netherlands and the discharge deficit of the Rhine are defined. Different probability distributions for the precipitation deficit are compared in Section 3. Section 4 presents probability distributions for the discharge deficit. The joint distribution of the precipitation and discharge deficits is discussed in Section 5. Return periods for joint exceedances estimated from the fitted bivariate distributions and from nearest-neighbor resampling are given for a number of extreme years in the historical record. In Section 6 the concept of a failure region, based on economic damage, as an alternative for the classic joint exceedance is discussed and illustrated with the same historical years. Section 7 concludes with a summary and a discussion of the results.

## 2. Drought Characteristics

[7] Two variables which describe drought in the Netherlands are considered here; the country average precipitation deficit and the discharge deficit of the Rhine River. The precipitation deficit is defined as the cumulative difference between precipitation and grass reference evaporation, from 1 April onward. When the precipitation deficit becomes negative it is reset to zero. The annual maximum precipitation deficit is the largest precipitation deficit that occurs during the summer half-year (April–September). Both for precipitation and evaporation daily values were available for the period 1906–2000, giving 95 independent annual maximum precipitation deficits. For practical reasons and for efficiency of the resampling procedure all daily data were converted into decades of days prior to the analysis. Decades of days were obtained by dividing each calendar month into three decades; the first two decades in a month always represent 10 days and the third decade represents the remaining days. Each year thus contains 36 decades of days.

[8] Average precipitation for the Netherlands was obtained by averaging the precipitation sums from 13 stations spread over the country. The grass reference evaporation was derived from temperature and sunshine duration at De Bilt using the Makkink formula [e.g., *de Bruin and Stricker*, 2000]. The global radiation in that formula was estimated from an empirical relation between global radiation and sunshine duration due to *Frantzen and Raaff* [1982]. Figure 1 presents time series of precipitation and estimated reference evaporation for the summer half-years of the period 1906–2000. From 1958 onward the values of the original Makkink evaporation are also given. It can be seen that these values are close to the estimates used in this study. For most years the reference evaporation is larger than precipitation, giving rise to a precipitation deficit. A precipitation deficit also builds up during dry periods in wet summer half-years. Figure 1 further shows that the driest years (1911, 1921, 1959 and 1976) have above normal reference evaporation.

[9] The discharge deficit of the Rhine River was based on discharge measurements at the German-Netherlands border (gauging station Lobith). Only decades for which the discharge was below a threshold of 1800 $m^3 s^{-1}$ contribute to the discharge deficit. For those decades the (nonnegative) difference between the threshold and the discharge is added to the discharge deficit. The discharge deficit was also calculated for the summer half-year and was available for the same period (1906–2000) as the precipitation deficit. A threshold of 1800 $m^3 s^{-1}$ roughly corresponds to the 20% quantile of the decade average discharge during the summer half-year. In 8 years the discharge is never below this threshold giving a zero discharge deficit. A lower threshold would result in many more years with a zero discharge deficit. Figure 2 presents time series of the maximum precipitation and discharge deficits for the period 1906–2000. No visible trends are found in these deficits during the

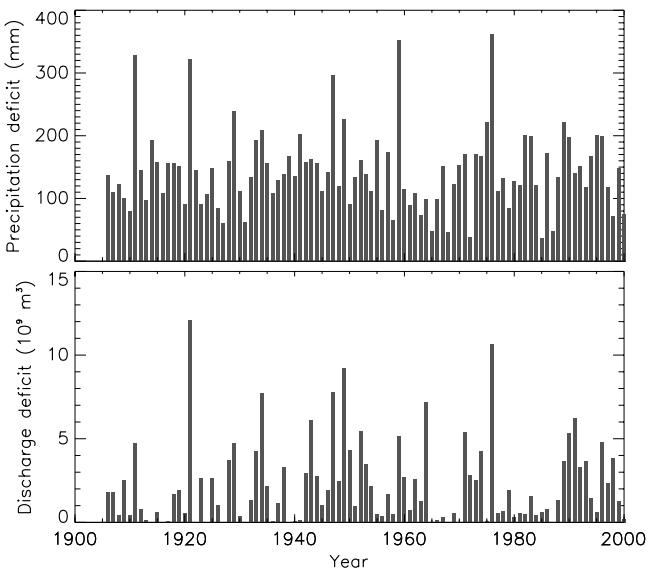


**Figure 2.** (top) Maximum precipitation deficit and (bottom) discharge deficit in the summer half-year (April–September) for the period 1906–2000.

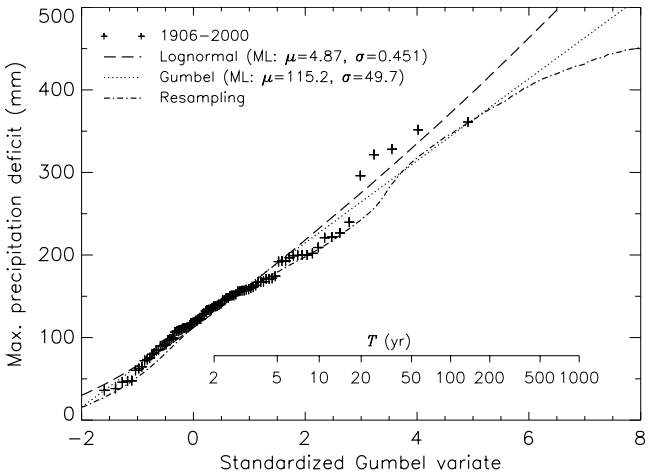


**Figure 3.** Ordered historical annual maximum precipitation deficits, the fitted Gumbel and lognormal distributions, and the simulated distribution from a resampling model. The parameters $\mu$ and $\sigma$ for the lognormal distribution refer to the mean and standard deviation of the underlying normal distribution.

past century. As expected, there is a positive correlation between the precipitation and discharge deficits.

## 3. Probability Distributions for the Precipitation Deficit

[10] Two distributions were fitted to the largest precipitation deficit in each year; the Gumbel distribution and the lognormal distribution, where the Gumbel distribution is given by

$$F(x) = \Pr(X \le x) = \exp\left[-e^{-(x-\mu)/\sigma}\right]. \quad (1)$$

The parameters of the distributions were estimated by the maximum likelihood (ML) method. In this section the fitted distributions are compared with a simulated distribution based on nearest-neighbor resampling of historical precipitation ($P$), evaporation ($E$) and discharge ($Q$) data. Conditions are imposed on the resampling process to reproduce the temporal dependence and the annual cycle of these variables as well as possible. A detailed description of the resampling model is given in Appendix A. With the resampling model, $10^5$ years (i.e., $36 \times 10^5$ decades) were simulated to empirically estimate the probability distribution of the (annual maxima of the) precipitation deficit and the discharge deficit. The simulated deficits are occasionally larger than those in the historical record as a result of reshuffling of the historical decade data (Appendix A).

[11] Figure 3 presents a Gumbel probability plot of the maximum precipitation deficits. The horizontal axis in this plot is chosen such that the Gumbel distribution corresponds to a straight line. It can be seen that the fitted lognormal distribution has a heavier upper tail than the fitted Gumbel distribution. If one is interested in the exceedance probabilities of the largest historical values, one might argue to use the lognormal distribution since this distribution performs best in this range of the data. The fitted distributions were subjected to the Anderson-Darling (A-D) test (as by *Stephens* [1986a]) and the "probability plot correlation coefficient" (ppcc) test [*Vogel*, 1986]. These tests were selected because they are known to be sensitive to deviations in the upper tail. Both tests give for the lognormal distribution a significant result at the 5% level, but not at the 1% level, while the Gumbel distribution passes both tests at the 5% level. Thus although the lognormal distribution describes the tail of the distribution better, these tests indicate that over the whole domain the lognormal distribution does not properly fit the data while the Gumbel distribution does.

[12] The curvature in the plot for the simulated data from the resampling model is more or less in agreement with that for the historical data, only the upper tail of the simulated distribution seems to be somewhat too light. The simulated distribution suggests that the precipitation deficit is limited which is true in fact. When there would be no precipitation at all during the summer half-year, the precipitation deficit is completely determined by the reference evaporation. Under present day climate conditions (in particular with respect to temperature and global radiation), the largest precipitation deficit is estimated to be 600 mm. For the fitted lognormal distribution (heaviest tail) a precipitation deficit of 600 mm is exceeded on average once in 2800 years.

## 4. Probability Distributions for the Discharge Deficit

[13] Probability distributions for the discharge deficit were obtained in a similar way as for the precipitation deficit. A Gumbel distribution was fitted to the annual discharge deficits. A sqrt-normal distribution (which assumes that the square root of the data are normally distributed) was also fitted. The choice of this distribution was based on the ML estimate of the optimal power transformation in the Box-Cox family [*Shumway et al.*, 1989].

[14] To avoid a large influence of small values of the discharge deficit on the estimated parameters the sample was censored at a low threshold of $0.03 \times 10^9$ m$^3$ in the fit of the sqrt-normal distribution and at $0.6 \times 10^9$ m$^3$ in the case of the Gumbel distribution. For data below the threshold only the information that they are smaller than the threshold is then used rather than their actual values. The parameters were estimated by the ML method (see, e.g., *Shumway et al.* [1989] for a transformed normal distribution and *Leese* [1973] for the Gumbel distribution).

[15] Figure 4 presents a Gumbel probability plot of the discharge deficits. For values larger than $1.0 \times 10^9$ m$^3$, the fitted Gumbel and sqrt-normal distributions are nearly indistinguishable. The simulated distribution from the resampling model agrees well with the two fitted distributions for return periods up to about 100 years. For longer return periods the simulated distribution starts to deviate. The discharge deficit is also bounded. Applying the lowest observed discharge (725 m$^3$ s$^{-1}$) to the whole summer half-year leads to a discharge deficit of $17 \times 10^9$ m$^3$. The largest historical discharge deficit (of 1921) amounts to 71% of this practical upper limit, and the largest simulated discharge deficits in the resampling model are about 85% of this limit.

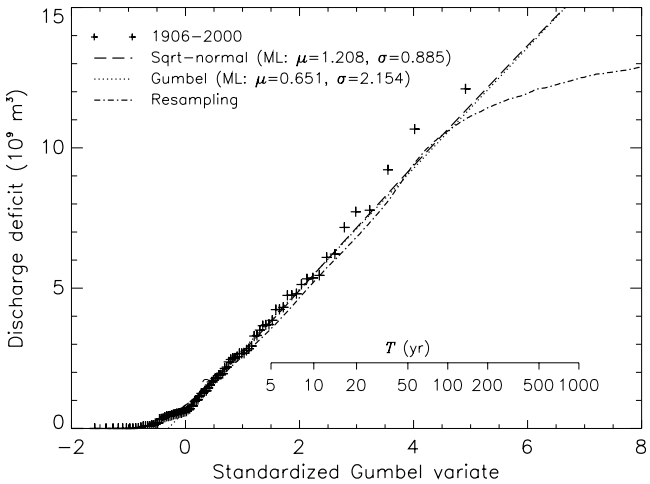


**Figure 4.** Ordered historical annual discharge deficits, the fitted Gumbel and sqrt-normal distributions, and the simulated distribution from a resampling model. The parameters μ and σ for the sqrt-normal distribution refer to the mean and standard deviation of the underlying normal distribution.

[16] Because of the censoring the goodness-of-fit tests used in the previous section can not be applied. Both the Gumbel and the sqrt-normal distribution pass the adapted ppcc test for censored data by *Stephens* [1986b] at the 5% level.

## 5. Bivariate Probability Distributions

[17] So far univariate probabilities have been considered. In the introduction it was noted that from a drought impacts point of view it is more interesting to look at joint exceedance probabilities. Drought events that have the largest economic impact are those events that have both a large precipitation deficit and a large discharge deficit. The latter makes compensation of the local water shortage by water from elsewhere in the Rhine basin very difficult.

[18] A logical way to proceed is to combine the univariate (marginal) probability distributions into a bivariate probability distribution. In the case that the maximum precipitation deficit is described by a lognormal distribution and the discharge deficit by a sqrt-normal distribution it would be natural to consider the bivariate normal distribution. The joint density of the standardized transformed precipitation and discharge deficits is then given by

$$\phi_2(x,y) = \frac{1}{2\pi\sqrt{1-\rho^2}} \exp\left[-\frac{1}{2(1-\rho^2)}\left(x^2 - 2\rho xy + y^2\right)\right], \quad (2)$$

where ρ is the correlation coefficient of the transformed values.

[19] A family of bivariate extensions of the Gumbel distribution is provided by the theory of multivariate extremes [e.g., *Tawn*, 1988; *Coles*, 2001]. This family can be represented as

$$F(x,y) = \Pr(X \le x, Y \le y) = \exp\left[-(e^{-x} + e^{-y})A\left(\frac{e^{-x}}{e^{-x} + e^{-y}}\right)\right], \quad (3)$$

where $A(\cdot)$ is the dependence function. $A(w) = 1$ implies that $X$ and $Y$ are independent, whereas $A(w) < 1$ implies that $X$ and $Y$ are positively associated ($0 < w < 1$). Perfect dependence, i.e., $\Pr(X = Y) = 1$, corresponds with $A(w) = \max[w, (1 - w)]$. Note that $A(0) = A(1) = 1$ both for independent and dependent Gumbel variables.

[20] Several parametric models for $A(w)$ have been proposed in the literature [e.g., *Kotz and Nadarajah*, 2000]. A popular one is the (symmetric) logistic dependence model:

$$A(w) = \left[w^{1/\alpha} + (1-w)^{1/\alpha}\right]^{\alpha}, 0 \le w \le 1; \quad 0 \le \alpha \le 1 \quad (4)$$

which leads to

$$F(x,y) = \exp\left[-\left(e^{-x/\alpha} + e^{-y/\alpha}\right)^{\alpha}\right], \quad (5)$$

where α characterizes the strength of the dependence between $X$ and $Y$; $\alpha = 1$ corresponds with independence and $\alpha = 0$ with perfect dependence. The correlation between $X$ and $Y$ equals $1 - \alpha^2$ [*Tiago de Oliveira*, 1980]. *Yue* [2001] used the logistic Gumbel model to describe the joint distribution of storm peaks and amounts and *Shiau* [2003] applied this model to extreme flood events (peaks and volumes).

[21] The dependence structure of the bivariate normal distribution differs from that of bivariate Gumbel distributions. A classical result for the bivariate normal distribution with $\rho < 1$ is that its components are asymptotically independent [*Sibuya*, 1960]. For the standard bivariate normal distribution in equation (2) asymptotic independence implies that

$$\lim_{u\to\infty} \Pr(Y > u | X > u) = 0. \quad (6)$$

A loose interpretation of this is that the probability that $Y$ is extreme given that $X$ is extreme tends to zero, or in other words, extreme values of $X$ and $Y$ do not occur simultaneously. For the bivariate logistic Gumbel distribution in equation (5), however, $\Pr(Y > u \mid X > u)$ tends to $2 - 2^{\alpha}$, and this distribution is therefore asymptotically dependent if $\alpha < 1$. Note that asymptotic dependence holds for all limiting bivariate extreme value distributions (including the logistic Gumbel distribution).

[22] In this section the dependence structure of the data is investigated first. Then the observed joint exceedance probabilities are compared with the theoretical ones from the bivariate models, and with those from the data simulated by nearest-neighbor resampling.

### 5.1. Dependence Structure

[23] Dependence measures for bivariate extremes have been discussed by *Coles et al.* [1999]. To remove the influence of the marginal distributions the variables $X$ and $Y$ are transformed to standard uniform variables, via $U = F_X(X)$ and $V = F_Y(Y)$. The joint distribution of $U$ and $V$ is called a copula. It contains all information about the association between $X$ and $Y$. Copulas have been applied recently in bivariate hydrological frequency analysis by *Favre et al.* [2004]. For the data $(x_i, y_i)$, $i = 1,\ldots, N$ the

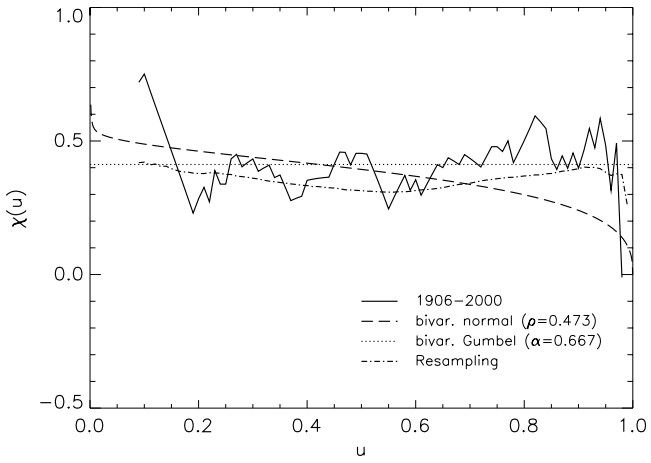


**Figure 5.** Dependence measure $\chi(u)$ for the historical and simulated data and for the fitted bivariate distributions. The value 0.667 for the parameter $\alpha$ in the bivariate Gumbel model corresponds to a correlation coefficient of 0.555.

influence of the marginal distributions can be removed in a similar way using the empirical distribution functions

$$u_i = \hat{F}_X(x_i) = \frac{\#\, x_j\text{s} \le x_i}{N+1}$$
$$v_i = \hat{F}_Y(y_i) = \frac{\#\, y_j\text{s} \le y_i}{N+1}. \tag{7}$$

*Buishand* [1984] introduced a measure of dependence to estimate the interstation dependence in the extremes of daily precipitation. A slight modification of this dependence measure is the quantity $\chi(u)$ suggested by *Coles et al.* [1999]:

$$\chi(u) = 2 - \frac{\ln \Pr(U < u, V < u)}{\ln \Pr(U < u)} \text{ for } 0 < u \le 1. \tag{8}$$

Independence corresponds with $\chi(u) = 0$ and perfect dependence with $\chi(u) = 1$. For the bivariate Gumbel distributions $\chi(u) = 2 - 2A(1/2)$, which reduces to $\chi(u) = 2 - 2^{\alpha}$ for the logistic dependence model. Further, for sufficiently large $u$,

$$\chi(u) \sim \Pr(V > u | U > u). \tag{9}$$

For asymptotically independent distributions like the bivariate normal distribution $\chi(u) \to 0$ as $u \to 1$. The measure $\chi(u)$ is not influenced by a monotonic increasing transformation of the data such as the log and sqrt transformation applied to the precipitation and discharge deficits to achieve normality.

[24] An empirical estimate of $\chi(u)$ can be constructed by substituting empirical estimates of the probabilities in the right-hand side of equation (8). Figure 5 presents such estimates of $\chi(u)$ for the historical and simulated data and the theoretical values for the fitted bivariate distributions. The parameters $\rho$ and $\alpha$ in these distributions were estimated by the ML method, taking into account the censoring of low discharge deficits (Appendix B). The figure shows that $\chi(u)$ is almost constant for the historical precipitation and discharge deficits. For the resampled data, the average level of $\chi(u)$ is slightly lower, with a weak minimum near $u = 0.5$. For large $u$, the estimates of $\chi(u)$ for the historical and the simulated data are more in line with the theoretical values for the bivariate Gumbel distribution than those for the bivariate normal distribution. For the latter $\chi(u)$ gradually decreases, but for $u$ near 1 it abruptly drops to zero. From a physical point of view, this behavior is not very realistic since a severe drought typically extends over a large area and will thus affect the precipitation in the Netherlands as well as in the upstream Rhine catchment. The use of the multivariate normal distribution to describe droughts over large geographic areas was already questioned by *Leytham* [1987]. He observed that this distribution underestimated the frequency of simultaneous low precipitation amounts or low river flows at widely separated sites.

[25] The question whether the data are asymptotically dependent or not can be investigated further by calculating for each year $T_i = \min(-1/\ln u_i, -1/\ln v_i)$. For large $z$, the probability that $T_i > z$ can be approximated by the Pareto distribution [*Ledford and Tawn*, 1996]:

$$\Pr(T_i > z) \approx c z^{-1/\eta}, \tag{10}$$

where $c$ and $\eta$ are the scale and shape parameters. For the bivariate Gumbel distribution $\eta = 1$, whereas for asymptotically independent data $\eta < 1$; $\eta = (\rho + 1)/2 = 0.74$ for the bivariate normal distribution. The parameter $\eta$ can be estimated from the $k$ largest values of $T_i$ using the ML method [*Hill*, 1975]. A quantile plot suggests that $k$ can be taken as large as 70. This results in $\hat{\eta} = 1.12$ with a standard error of 0.13, which supports the bivariate Gumbel distribution.

### 5.2. Symmetry of Dependence

[26] Both the bivariate normal distribution and the bivariate logistic Gumbel distribution have a symmetric dependence structure. Here symmetry implies that the dependence structure is such that the joint probabilities are unchanged when $X$ and $Y$ are interchanged. For a limiting bivariate Gumbel distribution this holds only if $A(w)$ is symmetrical about $w = 1/2$. This can be explored by estimating $A(w)$ with a nonparametric method. *Pickands* [1981] observed that $Z(w) = \min[e^{-X}/(1 - w), e^{-Y}/w]$ has an exponential distribution with mean $1/A(w)$, for each $w \in (0, 1)$. Transforming again the original variables to standard uniform variables, the following nonparametric estimate of $A(w)$ is obtained [*Hall and Tajvidi*, 2000]:

$$\hat{A}(w) = n\left[\sum_{i=1}^{n} Z_i(w)\right]^{-1}, \tag{11}$$

where

$$Z_i(w) = \min\left[\frac{\ln u_i}{(1-w)\overline{\ln u}}, \frac{\ln v_i}{w\overline{\ln v}}\right] \qquad (0 \le w \le 1),$$

with $(u_i, v_i)$ defined in equation (7) and $\overline{\ln u}$, $\overline{\ln v}$ the arithmetic means of $\{\ln u_i\}$, $\{\ln v_i\}$ respectively. For discharge deficits equal zero ($y_i = 0$), the numerator

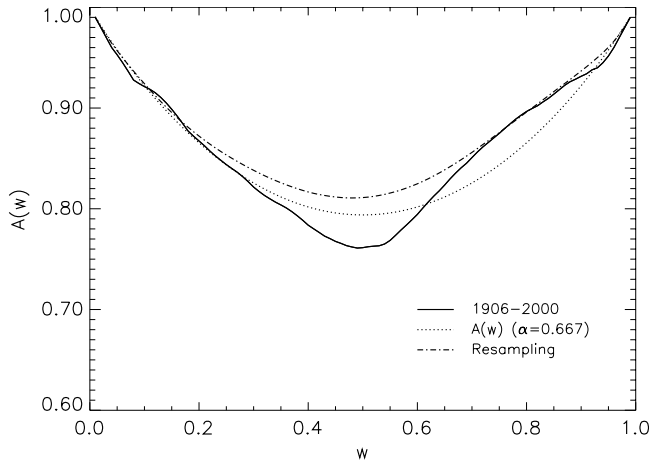


**Figure 6.** Nonparametric estimates of $A(w)$ from the historical and simulated data and $A(w)$ for the fitted logistic dependence model.

of $v_i$ in equation (7) is based here on their average rank, i.e., $[(\#\, y_j\text{s} = 0) + 1]/2$. Note that $\hat{A}(0) = \hat{A}(1) = 1$ (in agreement with $A(0) = A(1) = 1$).

[27] Figure 6 compares $\hat{A}(w)$ for the historical and simulated data with $A(w)$ for the fitted logistic dependence model. Apart from the bump around $w = 0.75$, which is partly due to the zero discharge deficits, $\hat{A}(w)$ is nearly symmetrical. The figure shows that the overall level of $\hat{A}(w)$ agrees with $A(w)$ for the logistic dependence model with $\alpha = 0.667$. The minimum of $\hat{A}(w)$ for the resampled data is somewhat larger than that of $A(w)$ but this is consistent with the lower average values of $\chi(u)$ for the resampled data in Figure 5.

### 5.3. Goodness of Fit

[28] In the previous subsections criteria were presented to discriminate between different models for the dependence between two random variables. To test the overall adequacy of a bivariate model, both the dependence structure and the fits of the individual marginal distributions should be taken into account. Here the goodness of fit of a bivariate model is assessed with joint exceedance probabilities. This is similar to *Yue et al.* [1999] and *Yue* [2001] who tested the validity of a bivariate model with empirical nonexceedance probabilities. Exceedance probabilities are preferred here because of the interest in discrepancies in the upper tail of the joint distribution.

[29] For each data pair $(x_i, y_i)$, a joint exceedance probability can be estimated as

$$\hat{p}(x_i, y_i) = \frac{\#\text{ pairs } (x_j, y_j) \text{ with } x_j \geq x_i \text{ and } y_j \geq y_i}{N+1}, \qquad (12)$$

and this can be compared with the theoretical value of $\Pr(X \geq x_i, Y \geq y_i)$ for the fitted bivariate model or a similar empirical estimate for the resampled data.

[30] Besides the bivariate normal distribution and the bivariate Gumbel distribution a novel bivariate distribution is considered, namely a bivariate normal distribution with a logistic Gumbel dependence structure. The latter is a logical combination of the other two bivariate distributions and it is constructed from the bivariate Gumbel model, using the transformations

$$\tilde{X} = \hat{H}_X^{-1}\left[\hat{G}_X(X)\right] \qquad \tilde{Y} = \hat{H}_Y^{-1}\left[\hat{G}_Y(Y)\right], \qquad (13)$$

where $\hat{G}_X$ and $\hat{G}_Y$ are the fitted Gumbel distributions, and $\hat{H}_X$, $\hat{H}_Y$ the fitted lognormal and sqrt-normal distributions, respectively. Since these transformations are monotonic increasing, $(\tilde{X}, \tilde{Y})$ has the same logistic dependence structure as $(X, Y)$. The transformations in equation (13) are similar to the normal quantile transformation by *Kelly and Krzysztofowicz* [1997]. The inverse of the normal quantile transform has been used to obtain variables having marginal extreme value distributions and a multivariate normal dependence structure [*Hosking and Wallis*, 1988; *Bortot et al.*, 2000]. Equation (13) is, however, needed if a logistic Gumbel dependence structure is required.

[31] Figure 7 shows joint probability plots for the three bivariate models and for the simulated data from the resampling model. To emphasize the upper tail, the exceedance probabilities are plotted on a logarithmic scale. In this tail region, the modeled probabilities tend to deviate systematically from the empirical probabilities, partly because these empirical probabilities are biased. The bias of $\hat{p}(x_i, y_i)$ depends on the degree of association of large values. From each bivariate distribution $10^4$ samples of 95 years were generated to explore this bias. Figure 8 shows the bias for the three bivariate distributions. The bias is identical for the bivariate Gumbel distribution and the bivariate normal distribution with logistic Gumbel dependence and somewhat larger for the bivariate normal distribution. By comparing Figures 7 and 8 it is clear that the observed differences between the modeled and empirical joint exceedance probabilities in the upper tail region (in Figure 7) are larger than the simulated bias (in Figure 8), in particular for the bivariate normal distribution and the resampling model. This lack of fit in the upper tail for the resampling model is mainly the result of light tails of the simulated marginal distributions (see Figures 3 and 4), and for the bivariate normal distribution it is due to its

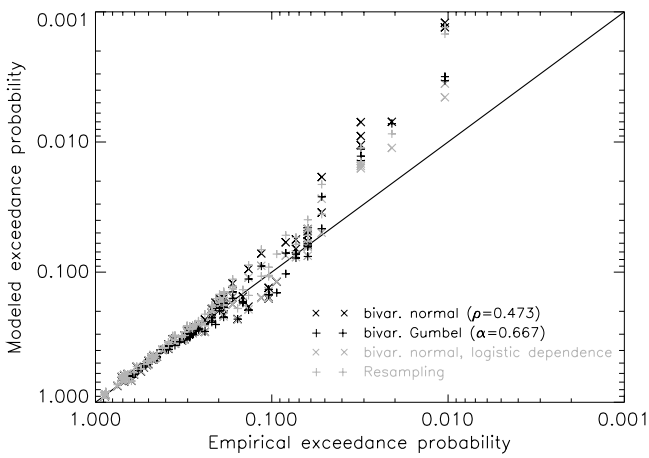


**Figure 7.** Joint probability plots for the fitted bivariate normal and Gumbel distributions, for the bivariate normal distribution with logistic Gumbel dependence structure, and for the data simulated with the resampling model. See color version of this figure at back of this issue.

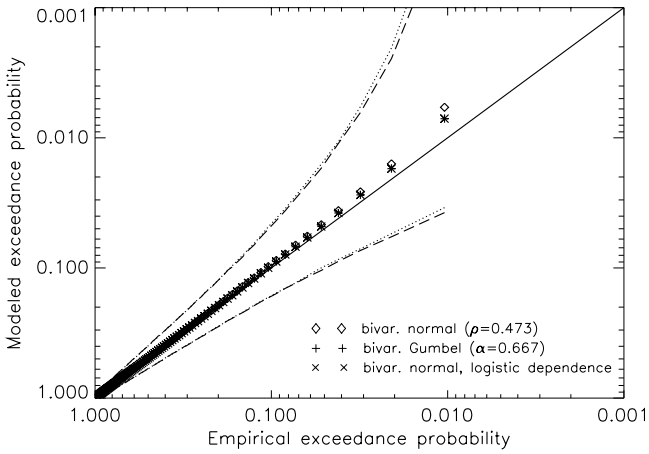


**Figure 8.** Bias of the empirical joint exceedance probabilities for the fitted bivariate normal and Gumbel distributions and for the bivariate normal distribution with logistic Gumbel dependence from a Monte Carlo experiment ($10^4$ simulations of 95 years). For each of the 95 empirical exceedance probabilities the symbols refer to the median value of the simulated theoretical exceedance probabilities, and the lines denote a pointwise 95% interval for the theoretical exceedance probabilities (dotted, bivariate normal; dashed, other).

asymptotic independence (Figure 5). Although all four models have a tendency to underestimate the joint exceedance probabilities in the upper tail region, the bivariate normal distribution with logistic Gumbel dependence performs best.

[32] For 5 extreme years in the historical record the return periods of joint exceedances of the observed precipitation and discharge deficit, i.e., $T = 1/\Pr(X > x_i, Y > y_i)$ were determined. Table 1 compares the estimates of $T$ from the different bivariate models.

[33] The return periods for the most extreme years (1921 and 1976) are more than 600 years for the bivariate normal distribution and the resampling model. These return periods reduce to less than 300 years if a bivariate normal distribution with logistic Gumbel dependence structure is assumed. Apart from a large sensitivity to model choice, the return periods are very uncertain due to sampling variability (see, for the univariate case, *Stedinger et al.* [1993]). Yet this does not entirely explain why the estimates in Table 1 considerably exceed the length of the historical records from which they were derived. An important point is that the probability that two different variables exceed some high level simultaneously is smaller than the marginal exceedance probabilities for each of the two variables. The magnitude of this effect can be estimated from the same Monte Carlo experiment that was used to determine the bias of $\hat{p}(x_i, y_i)$. For each 95 year sample from the normal distribution with logistic dependence, the return periods of the joint exceedances of the simulated precipitation and discharge deficits were determined. The median of the longest return period in the $10^4$ simulations of 95 years is 320 years which is quite large compared to the size of the sample. As a result of this effect all 5 years considered in Table 1 have return periods longer than 60 years.

## 6. Failure Regions

[34] In practical applications, the joint probability that $X$ and $Y$ lie in a "failure region" different from the rectangle defined by ($X > x$, $Y > y$) might be of interest. For example, structures often fail if a combination of the constituent variables becomes extreme. This combination then marks the boundary of the failure region. For the assessment of droughts in the Netherlands it is useful to base the failure region on the economic damage $D_E$.

[35] The economic damage from 7 historical years (1949, 1959, 1967, 1976, 1985, 1995 and 1996 (T. Kroon, personal communication, 2004)) reveals that $D_E$ can be approximated as

$$D_E = ax + by + c, \tag{14}$$

with $x$ the maximum precipitation deficit and $y$ the discharge deficit. The regression coefficients $a$, $b$ and $c$ were estimated by a least squares fit. Let $x_i$ and $y_i$ be the observed precipitation and discharge deficits for the year of interest. Events with a precipitation and discharge deficit in the region above the line through ($x_i$, $y_i$) and with slope $\Delta = -a/b$ should then be considered as more extreme in terms of economic damage. For the years 1976, 1959 and 1949, Figure 9 compares the boundary of this failure region with the rectangle ($X > x_i$, $Y > y_i$). The slope of the bounding line indicates that the economic damage is relatively more sensitive to the precipitation deficit. Table 2 presents, for each of the historical years in Table 1, the return periods for the failure region based on equation (14). These return periods were obtained empirically from $10^6$ simulated pairs ($x_i$, $y_i$) from the corresponding bivariate distribution and from the $10^5$ simulated years in the case of nearest-neighbor resampling.

[36] The estimated return periods in Table 2 are much shorter than those in Table 1, in particular for 1921 and 1976. Using a failure region related to the economic damage gives the longest return period for 1976 while in Table 1 the

**Table 1.** Mean Return Periods of Joint Exceedances of the Observed Precipitation and Discharge Deficits in Given Years for Different Bivariate Distributions and the Resampling Model[a]

| Year | Precipitation Deficit, mm | Discharge Deficit, $10^9$ m$^3$ | Normal | Gumbel | Normal, Logistic Dependence | Resampling |
|---|---|---|---|---|---|---|
| 1921 | 321.6 | 12.1 | 824 | 318 | 281 | 757 |
| 1976 | 361.1 | 10.7 | 760 | 296 | 221 | 676 |
| 1959 | 351.7 | 5.1 | 143 | 139 | 90 | 116 |
| 1947 | 296.1 | 7.8 | 142 | 78 | 65 | 90 |
| 1949 | 226.7 | 9.2 | 111 | 72 | 68 | 68 |

[a]Return period is in years.

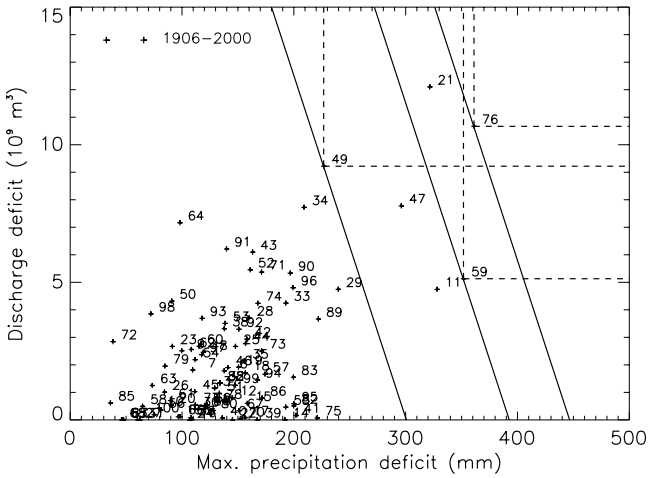


**Figure 9.** Failure regions related to the economic damage (equation (14)) and rectangles ($X > x_i$, $Y > y_i$) for the historical years 1976, 1959, and 1949 (indicated as 76, 59, and 49).

longest return period is found for 1921. This is a result of the relatively smaller contribution of the discharge deficit to the economic damage (see Figure 9). In Table 1 the return periods are longest for the bivariate normal distribution while in Table 2 the longest return periods are found for the bivariate Gumbel distribution and the resampling model. The shortest return periods are found in both tables for the bivariate normal distribution with logistic Gumbel dependence, but the difference from the standard bivariate normal distribution is much smaller in Table 2. This is in line with results of *Tawn* [1988] and *Coles and Tawn* [1994] that the sensitivity of joint probabilities to assumptions about the dependence structure varies considerably with the type of failure region. For the best fitting model (bivariate normal distribution with logistic dependence), the estimated return period of 110 years for the most extreme year in terms of economic damage, 1976, is close to the length of the historical record. In contrast to the return periods in Table 1, the estimates in Table 2 can be considered as a univariate exceedance probability, namely that for the economic damage $D_E$.

[37] Although the regression coefficients in equation (14) differ significantly from zero at the 10% level, the slope $\Delta$ is quite uncertain. To determine the effect of this uncertainty on the estimated return periods, the latter were recalculated with the 5th percentile $\Delta_L$ and the 95th percentile $\Delta_U$ of the empirical distribution of the estimated slope in $10^4$ bootstrap samples of size 7. The resulting spread in the return periods is presented in Figure 10. For 1959, a year with a relatively small discharge deficit, a failure region with slope $\Delta_L$ leads to a longer return period and a region with slope $\Delta_U$ shortens the return period, while for the other years in Table 2 the return periods change the other way round. Within the uncertainty of $\Delta$, 1976 always has the largest economic damage and thus the longest return period. However, 1959 becomes more extreme than 1921 if the failure region has slope $\Delta_L$ and it becomes less extreme than 1947 if the failure region has slope $\Delta_U$. So the ranking of the drought events also depends on the slope of the failure region.

## 7. Discussion and Conclusions

[38] Different probability distributions have been fitted to the annual maximum precipitation deficit in the Netherlands and the annual discharge deficit of the Rhine River. The fitted distributions have been compared with an empirical bivariate distribution obtained with a resampling model. It is found that the degree of association between large values is too weak if the dependence structure of a bivariate normal distribution is assumed. This results in a strong underestimation of the probabilities of joint exceedances of extreme values. The joint occurrence of large values is better described by the dependence structure of a limiting Gumbel distribution. Its symmetric nature is also in agreement with the data. This dependence function has therefore not only been studied with Gumbel marginals but also with transformed normal marginals. The latter describes the upper tail of the precipitation deficit distribution better, leading to shorter return periods between extreme bivariate events than the Gumbel distribution. The assumption of Gumbel marginals is, however, not rejected by the Anderson-Darling and the ppcc tests. For the resampling model the dependence structure and its symmetry agree well with the data. The resampling model is the only model which can (to some extent) reproduce the curvature in the tail of the historical distribution of the maximum precipitation deficit, although it underestimates the most extreme quantiles of this distribution. The tail of the simulated distribution of the discharge deficit seems too light as well, in particular near the most extreme event (1921). This discrepancy seems to be related with differences in the strength of the autocorrelation between the variables $E - P$ and $Q$. Decade values of $E - P$ exhibit only weak autocorrelation whereas for discharge $Q$ there is still considerable autocorrelation at a lag of 10 decades (see Appendix A). A much better simulation of the upper

**Table 2.** Mean Return Periods (yr) of Situations Where the Precipitation and Discharge Deficits are More Extreme Than the Observed Deficits in the Given Years in Terms of Economic Damage (Equation (14)) for the Different Bivariate Distributions and the Resampling Model[a]

| Year | Precipitation Deficit, mm | Discharge Deficit, $10^9$ m$^3$ | Normal | Gumbel | Normal, Logistic Dependence | Resampling |
|---|---|---|---|---|---|---|
| 1921 | 321.6 | 12.1 | 99 | 113 | 79 | 98 |
| 1976 | 361.1 | 10.7 | 147 | 172 | 110 | 178 |
| 1959 | 351.7 | 5.1 | 66 | 75 | 55 | 67 |
| 1947 | 296.1 | 7.8 | 41 | 46 | 36 | 46 |
| 1949 | 226.7 | 9.2 | 17 | 19 | 17 | 24 |

[a]Return period is in years.

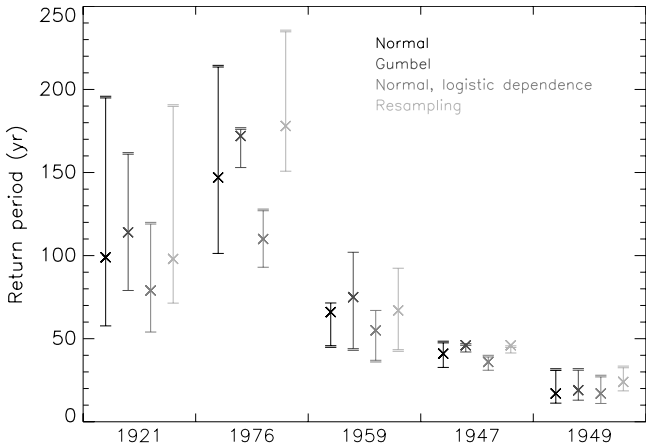


**Figure 10.** Spread in return periods due to the uncertainty of the failure region slope Δ. The single horizontal bars correspond with $\Delta_L$, the double horizontal bars correspond with $\Delta_U$, and the crosses (×) correspond with the return periods in Table 2. See color version of this figure at back of this issue.

tails of the marginal distributions can be achieved when $E - P$ and $Q$ are resampled individually rather than simultaneously. This is, however, not of interest for the estimation of the drought probabilities considered in this study.

[39] The use of a failure region based on economic damage has been studied as an alternative to ordinary joint exceedances. This failure region not only shortens the estimated return periods of historical drought events, it also reduces the differences between the various bivariate models. For the most extreme year in terms of economic damage, 1976, the return period is 172 years for the bivariate Gumbel distribution, 110 years for the transformed normal distribution with logistic Gumbel dependence and 178 years for nearest-neighbor resampling. A detailed study of the uncertainty of these return periods was beyond the scope of this paper, but the uncertainty is related to incomplete knowledge of the shape of the upper tail of the joint distribution, the limited sample size, and the uncertainty in the slope of the failure region. The size of the latter uncertainty depends on the type of distribution and may vary considerably from year to year (Figure 10).

## Appendix A

### A1. Nearest-Neighbor Resampling

[40] In the nearest-neighbor method the variables of interest are sampled simultaneously with replacement from the historical data. To incorporate temporal correlation, resampling is restricted to the historical values that have similar characteristics as those of the last simulated decade. One of these nearest neighbors or analogs is randomly selected and its historical successor is the next simulated decade.

[41] A feature vector (or state vector) $\mathbf{D}_t$ is used to find the nearest neighbors in the historical data. $\mathbf{D}_t$ is formed from standardized (weather) variables generated for decade $t - 1$ and earlier decades. The latter is necessary to reproduce longer-term variability [e.g., *Harrold et al.*, 2003a, 2003b]. The nearest neighbors of $\mathbf{D}_t$ are selected in terms of a weighted Euclidean distance. For two $q$-dimensional vectors $\mathbf{D}_t$ and $\mathbf{D}_u$ this distance is defined as

$$\delta(\mathbf{D}_t, \mathbf{D}_u) = \left( \sum_{j=1}^{q} w_j \left( v_{tj} - v_{uj} \right)^2 \right)^{\frac{1}{2}}, \tag{A1}$$

where $v_{tj}$ and $v_{uj}$ are the $j$th components of $\mathbf{D}_t$ and $\mathbf{D}_u$ respectively and the $w_j$s are scaling weights. To obtain an equal contribution of all feature vector elements to the Euclidean distance, the weights $w_j$ are inversely proportional to the variance of those elements. The weights are calculated separately for each of the 36 calendar decades to account for the seasonal variation in the variance. A decreasing kernel [*Lall and Sharma*, 1996] is used to select one of the $k$ nearest neighbors:

$$p_j = \frac{1/j}{\sum_{i=1}^{k} 1/i}, \quad j = 1, .., k, \tag{A2}$$

with $p_j$ the probability that the $j$th closest neighbor is resampled, and $k = 5$ [*Buishand and Brandsma*, 2001]. To impose a realistic seasonal cycle upon the simulated data the search for nearest neighbors was restricted to a 7 decade wide "moving window," centered on the calendar decade to be simulated. This window prevents that "summer decades" are simulated during winter and "winter decades" during summer [*Buishand and Brandsma*, 2001]. For the historical record of 95 years, the nearest neighbors are thus selected from $7 \times 95 = 665$ decades.

[42] A resampling technique cannot produce smaller or larger decade values than those found in the historical record. However, for periods longer than a decade, the precipitation or discharge deficit can be larger than the largest historical deficit because of rearranging extreme decade values from different parts of the historical record. In fact, this is the property that can make resampling methods useful. In a number of simulation studies of daily precipitation the generated extreme multiday precipitation amounts were well beyond the extreme historical amounts and followed a Gumbel distribution, even outside the range of the historical data [*Brandsma and Buishand*, 1998; *Wójcik and Buishand*, 2003].

### A2. Model Identification

[43] Since the objective of the resampling model is to simulate values of precipitation $P$, evaporation $E$ and discharge $Q$ simultaneously, certain characteristics of these variables should be included in the feature vector. Several simulations were performed with different feature vectors. Best results, regarding the upper tails of the distributions of both the precipitation deficit and the discharge deficit (Figures 3 and 4) are obtained when the feature vector contains the following three elements: (1) the standardized discharge ($Q$) of the latest simulated decade, (2) the average standardized discharge during the previous 18 decades, and (3) the average of the standardized difference between precipitation and evaporation ($E - P$) in the 13 decades prior to the decade of interest. The discharge was standardized by dividing by the mean

discharge for the calendar decade of interest. The variable $E - P$ was standardized by subtracting the mean and dividing by the sample standard deviation for the calendar decade of interest.

[44] Besides the model presented in this study also models with $Q$, $E$ and $P$ as individual feature vector elements, and models with different memory lengths (ranging between 2 and 12 months) were investigated but all of them gave poorer results.

### A3. Model Results

[45] To give an impression of the model performance, Table A1 compares the average values and the standard deviations of evaporation minus precipitation ($E - P$) and of the Rhine discharge ($Q$) for the summer half-year in the simulated series with those in the historical series.

[46] The averages and the standard deviations at various timescales in the simulated data are generally within one standard error from those in the historical data, pointing to a good correspondence between the simulated and historical data.

[47] Figure A1 presents, also for the summer half-year, the autocorrelation functions of $E - P$ and $Q$ for the historical and simulated data. As expected, the autocorrelation is much larger for the Rhine discharge ($Q$) than for $E - P$. For all lags the autocorrelation of $Q$ is very well reproduced by the resampling model. For $E - P$ the lag 1 autocorrelation is somewhat underestimated while the lag 2 autocorrelation is slightly overestimated. Overall, the autocorrelation functions are well reproduced by the resampling model.

## Appendix B: Maximum Likelihood Estimation of the Dependence Parameters ρ and α

[48] The estimation of the dependence parameters for the bivariate distributions was carried out after the estimation of the marginal distributions. The likelihood is then based on the joint distribution of the standardized data, i.e., equation (2) for the bivariate normal distribution and equation (5) for the bivariate logistic Gumbel distribution. The standardized data are denoted as $(x_1, y_1)$, $(x_2, y_2)$,. . ., $(x_N, y_N)$.

[49] Censoring was necessary to estimate the parameters of the marginal distributions for the discharge deficit (Section 4). Let $y_{n+1} < t$, $y_{n+2} < t$,. . ., $y_N < t$ correspond to the censored data. The likelihood for the parameter $\alpha$ in the logistic dependence model is then given by [*Smith*, 1994; *Ledford and Tawn*, 1996; *Coles*, 2001]:

$$L(\alpha) = \prod_{i=1}^{n} f(x_i, y_i) \prod_{i=n+1}^{N} \left.\frac{\partial F}{\partial x}\right|_{(x_i,t)}, \tag{B1}$$

where $f(x, y) = \frac{\partial^2 F}{\partial x \partial y}$ is the joint density:

$$\begin{aligned} f(x,y) = {} & e^{-(x+y)/\alpha} \left(e^{-x/\alpha} + e^{-y/\alpha}\right)^{\alpha-2} \\ & \times \left[\left(e^{-x/\alpha} + e^{-y/\alpha}\right)^{\alpha} + 1/\alpha - 1\right] \\ & \times \exp\left[-\left(e^{-x/\alpha} + e^{-y/\alpha}\right)^{\alpha}\right]. \end{aligned} \tag{B2}$$

[50] For the bivariate normal distribution the likelihood (B1) can be written

$$L(\rho) = \prod_{i=1}^{n} \phi_2(x_i, y_i) \prod_{i=n+1}^{N} \Pr(Y \le t | X = x_i)\phi(x_i), \tag{B3}$$

where $\phi(x)$ is the standard normal density. Because the conditional distribution of $Y$ in equation (B3) is normal with mean $\rho x_i$ and variance $1 - \rho^2$, the likelihood becomes

$$L(\rho) = \prod_{i=1}^{n} \phi_2(x_i, y_i) \prod_{i=n+1}^{N} \Phi\left(\frac{t - \rho x_i}{\sqrt{1-\rho^2}}\right)\phi(x_i), \tag{B4}$$

with $\Phi(x) = \int_{-\infty}^{x} \phi(x)\mathrm{d}x$ the distribution function of a standard normal variable.

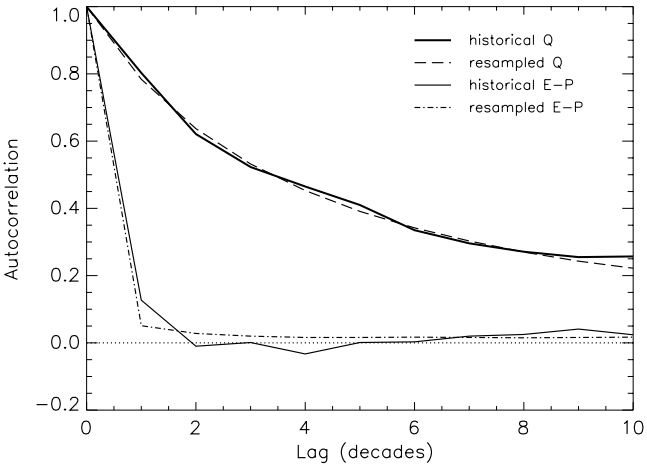


**Figure A1.** Autocorrelation functions of $E - P$ and $Q$ for the historical and simulated data.

**Table A1.** Averages and Standard Deviations of Evaporation Minus Precipitation ($E - P$) and of the Rhine Discharge ($Q$) in the Historical Records and the Simulated Series for the Summer Half-Year (April–September)[a]

| | Historical | | Simulated | |
|---|---|---|---|---|
| | $E - P$ | $Q$ | $E - P$ | $Q$ |
| Average | 4.1 (0.5) | 2114 (50) | 3.7 | 2117 |
| $\sigma_{decade}$ | 18.7 (0.4) | 731 (33) | 18.6 | 720 |
| $\sigma_{month}$ | 11.7 (0.4) | 657 (31) | 11.2 | 652 |
| $\sigma_{summer}$ | 5.2 (0.5) | 488 (33) | 5.2 | 472 |

[a] $E - P$ is in mm decade$^{-1}$, and $Q$ is in m$^3$ s$^{-1}$. For the historical data the standard errors are given between parentheses. The standard errors of the standard deviations were calculated following *Buishand and Beersma* [1996] and *Beersma and Buishand* [1999].

[51] **Acknowledgments.** The authors thank two anonymous reviewers and an Associate Editor for their comments on an earlier version of the paper. The work was performed in the framework of the "Drought studies of the Netherlands" in cooperation with the Institute for Inland Water Management and Waste Water Treatment (RIZA), Lelystad.

## References

Beersma, J. J., and T. A. Buishand (1999), A simple test for equality of monthly variances in climate time series, *J. Clim.*, *12*, 1770–1779.

Bortot, P., S. G. Coles, and J. A. Tawn (2000), The multivariate Gaussian tail model: An application to oceanographic data, *Appl. Stat.*, *49*, 31–49.

Brandsma, T., and T. A. Buishand (1998), Simulation of extreme precipitation in the Rhine basin by nearest-neighbour resampling, *Hydrol. Earth Syst. Sci.*, *2*, 195–209. (Corrigendum, *Hydrol. Earth Syst. Sci.*, *3*, 319, 1999.)

Buishand, T. A. (1984), Bivariate extreme-value data and the station-year method, *J. Hydrol.*, *69*, 77–95.

Buishand, T. A., and J. J. Beersma (1996), Statistical tests for comparison of daily variability in observed and simulated climates, *J. Clim.*, *9*, 2538–2550. (Corrigendum, *J. Clim.*, *10*, 818 1997.)

Buishand, T. A., and T. Brandsma (2001), Multisite simulation of daily precipitation and temperature in the Rhine basin by nearest-neighbor resampling, *Water Resour. Res.*, *37*, 2761–2776.

Coles, S. G. (2001), *An Introduction to Statistical Modeling of Extreme Values*, Springer-Verlag, New York.

Coles, S. G., and J. A. Tawn (1994), Statistical methods for multivariate extremes: An application to structural design (with discussion), *Appl. Stat.*, *43*, 1–48.

Coles, S. G., J. E. Heffernan, and J. A. Tawn (1999), Dependence measures for multivariate extremes, *Extremes*, *2*, 339–365.

de Bruin, H. A. R., and J. N. M. Stricker (2000), Evaporation of grass under non-restricted soil moisture conditions, *Hydrol. Sci. J.*, *45*, 391–406.

Favre, A.-C., S. El Adlouni, L. Perreault, N. Thiémonge, and B. Bobée (2004), Multivariate hydrological frequency analysis using copulas, *Water Resour. Res.*, *40*, W01101, doi:10.1029/2003WR002456.

Frantzen, A. J., and W. R. Raaff (1982), The relation between global radiation and relative sunshine duration in the Netherlands (in Dutch), *Sci. Rep. W. R. 82-5*, R. Neth. Meteorol. Inst., De Bilt, Netherlands.

Hall, P., and N. Tajvidi (2000), Distribution and dependence-function estimation for bivariate extreme-value distributions, *Bernoulli*, *6*, 835–844.

Harrold, T. I., A. Sharma, and S. J. Sheather (2003a), A nonparametric model for stochastic generation of daily rainfall occurrence, *Water Resour. Res.*, *39*(10), 1300, doi:10.1029/2003WR002182.

Harrold, T. I., A. Sharma, and S. J. Sheather (2003b), A nonparametric model for stochastic generation of daily rainfall amounts, *Water Resour. Res.*, *39*(12), 1343, doi:10.1029/2003WR002570.

Hill, B. M. (1975), A simple general approach to inference about the tail of a distribution, *Ann. Stat.*, *3*, 1163–1174.

Hosking, J. R. M., and J. R. Wallis (1988), The effect of intersite dependence on regional flood frequency analysis, *Water Resour. Res.*, *24*, 588–600.

Kelly, K. S., and R. Krzysztofowicz (1997), A bivariate meta-Gaussian density for use in hydrology, *Stochastic Hydrol. Hydraul.*, *11*, 17–31.

Kotz, S., and S. Nadarajah (2000), *Extreme Value Distributions: Theory and Applications*, Imperial Coll. Press, London.

Kroll, C. N., and J. R. Stedinger (1998), Regional hydrologic analysis: Ordinary and generalized least squares revisted, *Water Resour. Res.*, *34*, 121–128.

Lall, U., and A. Sharma (1996), A nearest neighbor bootstrap for resampling hydrologic time series, *Water Resour. Res.*, *32*, 679–693.

Ledford, A., and J. A. Tawn (1996), Statistics for near independence in multivariate extreme values, *Biometrika*, *83*, 169–187.

Leese, M. N. (1973), Use of censored data in the estimation of Gumbel distribution parameters for annual maximum flood series, *Water Resour. Res.*, *9*, 1534–1542.

Leytham, K. M. (1987), A joint rank test for assessing multivariate normality in hydrologic data, *Water Resour. Res.*, *23*, 2311–2317.

Middelkoop, H., and C. O. G. van Haselen (1999), Twice a river: Rhine and Meuse in the Netherlands, *Rep. 99.003*, RIZA, Arnhem, Netherlands.

Pickands, J. (1981), Multivariate extreme value distributions, *Bull. Int. Stat. Inst.*, *49*, 859–878.

Rajagopalan, B., and U. Lall (1999), A k-nearest-neighbor simulator for daily precipitation and other weather variables, *Water Resour. Res.*, *35*, 3089–3101.

Shiau, J. T. (2003), Return period of bivariate distributed extreme hydrological events, *Stochastic Environ. Res. Risk Assess.*, *17*, 42–57.

Shumway, R. H., A. S. Azari, and P. Johnson (1989), Estimating mean concentrations under transformation for environmental data with detection limits, *Technometrics*, *31*, 347–356.

Sibuya, M. (1960), Bivariate extreme statistics, *Ann. Inst. Stat. Math.*, *11*, 195–210.

Smith, R. L. (1994), Multivariate threshold methods, in *Extreme Value Theory and Application*, edited by J. Galambos, J. Lechner, and E. Simiu, pp. 225–248, Kluwer Acad., Norwell, Mass.

Stedinger, J. R., R. M. Vogel, and E. Foufoula-Georgiou (1993), Frequency analysis of extreme events, in *Handbook of Hydrology*, edited by D. Maidment, pp. 18.1–18.66, McGraw-Hill, New York.

Stephens, M. A. (1986a), Tests based on EDF statistics, in *Goodness-of-Fit Techniques*, edited by R. B. D'Agostino and M. A. Stephens, pp. 97–193, Marcel Dekker, New York.

Stephens, M. A. (1986b), Tests based on regression and correlation, in *Goodness-of-Fit Techniques*, edited by R. B. D'Agostino and M. A. Stephens, pp. 195–233, Marcel Dekker, New York.

Tawn, J. A. (1988), Bivariate extreme value theory: Models and estimation, *Biometrika*, *75*, 397–415.

Tiago de Oliveira, J. (1980), Bivariate extremes: Foundations and statistics, in *Multivariate Analysis*, vol. 5, edited by P. R. Krishnaiah, pp. 349–366, North-Holland, New York.

Vogel, R. M. (1986), The probability plot correlation test for the normal, lognormal, and Gumbel distributional hypotheses, *Water Resour. Res.*, *22*, 587–590.

Wójcik, R., and T. A. Buishand (2003), Simulation of 6-hourly rainfall and temperature by two resampling schemes, *J. Hydrol.*, *273*, 69–80.

Young, K. C. (1994), A multivariate chain model for simulating climatic parameters from daily data, *J. Appl. Meteorol.*, *33*, 661–671.

Yue, S. (2001), The Gumbel logistic model for representing a multivariate storm event, *Adv. Water Resour.*, *24*, 179–185.

Yue, S., T. B. M. J. Ouarda, B. Bobée, P. Legendre, and P. Bruneau (1999), The Gumbel mixed model for flood frequency analysis, *J. Hydrol.*, *226*, 88–100.

J. J. Beersma and T. A. Buishand, Royal Netherlands Meteorological Institute, P.O. Box 201, N-3730AE De Bilt, Netherlands. (jules.beersma@knmi.nl; adri.buishand@knmi.nl)

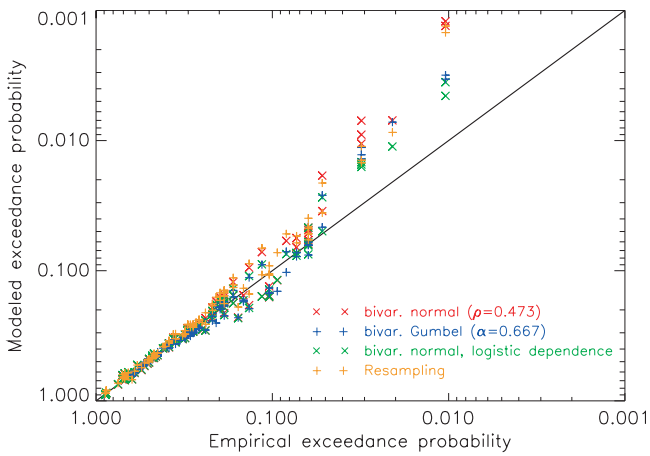


**Figure 7.** Joint probability plots for the fitted bivariate normal and Gumbel distributions, for the bivariate normal distribution with logistic Gumbel dependence structure, and for the data simulated with the resampling model.

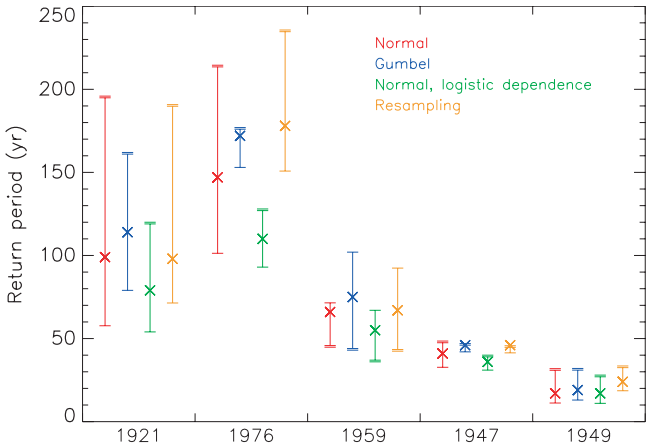


**Figure 10.** Spread in return periods due to the uncertainty of the failure region slope Δ. The single horizontal bars correspond with $\Delta_L$, the double horizontal bars correspond with $\Delta_U$, and the crosses (×) correspond with the return periods in Table 2.